Kinetic characteristics of *Escherichia coli* RNase H1: cleavage of various antisense oligonucleotide–RNA duplexes

Stanley T. CROOKE,* Kristina M. LEMONIDIS, Lorna NEILSON, Richard GRIFFEY, Elena A. LESNIK and Brett P. MONIA
Isis Pharmaceuticals, Inc., Carlsbad, CA 92008, U.S.A.

1. The effects of variations in substrates on the kinetic properties of *Escherichia coli* RNase H were studied using antisense oligonucleotides of various types hybridized to complementary oligoribonucleotides. The enzyme displayed minimal sequence preference, initiated cleavage through an endonucleolytic mechanism near the 3′ terminus of the RNA in a DNA–RNA chimera and then was processively exonucleolytic. Phosphorothioate oligodeoxynucleotides hybridized to RNA supported cleavage more effectively than phosphodiester oligodeoxynucleotides. Oligonucleotides comprised of 2′-methoxy-, 2′-fluoro- or 2′-propoxy-nucleosides did not support RNase H1 activity. 2. The K_m and $V_{max.}$ of cleavage of RNA duplexes with full phosphorothioate oligodeoxynucleotides were compared with methoxydeoxy 'gapmers', i.e.; oligonucleotides with 2′-methoxy wings surrounding a deoxynucleotide centre. Such structural modifications resulted in substantial increases in affinity, but significant reductions in cleavage efficiency. The initial rates of cleavage increased as the deoxynucleotide gap size was increased. Multiple deoxynucleotide gaps increased the $V_{max.}$ but had little effect on K_m. 3. The effects of several base modifications on the site of initial cleavage, processivity and initial rate of cleavage were also studied.

INTRODUCTION

Ribonuclease H (RNase H)-type enzymes selectively cleave the RNA strand of an RNA–DNA duplex through an endonucleolytic mechanism (for review, see [1]). RNase H-type activity has been demonstrated for a growing, relatively large family of proteins. In *Escherichia coli*, there are at least two RNase H isotypes expressed from separate genes [2]. Enzymes with similar activities have been identified in a number of other bacteria [3–12], yeast [6], trypanosomes [7], calf thymus [8,9] and other mammalian cells [3–12].

E. coli RNase H1 has been crystallized [13–16] and the substrate specificity and kinetic properties of *E. coli* RNase H1 have been studied. The preferred substrate is clearly an RNA–DNA duplex. In the RNA strand, both the 2′-OH and the phosphate groups are essential [17,18]. In the DNA strand, 2′-methoxy modifications have been reported to eliminate the activity of the enzyme [19–22] and substitution of the uncharged methylphosphonate group for the phosphate resulted in a substrate that was not cleaved by the enzyme [18]. In contrast, although at high concentrations phosphorothioate oligodeoxynucleotides inhibit the enzyme, they serve as effective substrates when in an RNA–DNA duplex [23]. Interestingly, in one report of a study on human RNase H1, the substitution of a ribonucleotide in the deoxynucleotide strand supported cleavage at the nucleotide hybridized to the ribonucleotide [19].

Both HIV reverse transcriptase and *E. coli* RNase H1 have been reported to be 'processive endonucleases'; that is, they induce cleavage endonucleolytically at a nucleotide involved in a DNA–RNA hybrid, then processively induce 3′–5′ exonucleolytic cleavage [20].

Kinetic analyses of *E. coli* RNase H1-mediated cleavage have been reported for wild-type and mutant enzymes using full DNA–RNA duplexes [16] and for wild-type enzyme using duplexes comprised of one strand of DNA and one strand containing a short RNA segment flanked by DNA regions [21]. Using the former substrate, the K_m and $V_{max.}$ reported were 0.11 μM and 36 units/mg of protein respectively, where 1 unit of activity equalled 1 μmol of acid-soluble material per min. Using the latter substrate, the predominant cleavage site was just before the second ribonucleotide from the 3′ RNA–DNA junction and the K_m was 4.2 μM.

The effects of altering the regions that flank the site of cleavage of the RNA substrate on the RNA strand have been studied to some extent, but detailed kinetic studies have not been reported. Using an RNA gap of various lengths (3–6 nucleotides), and a DNA duplex, Hogrefe et al. [21] concluded that increasing the size of the RNA gap decreased the K_m, but that maximal turnover occurred with the 4-base RNA gaps. Furthermore, replacing the flanking RNA with 2′-methoxynucleotides had no negative effect on the cleavage of the ribonucleotide gap.

Arguably, a more pharmacologically relevant approach is to vary the chemical characteristics of the hybridizing oligonucleotide rather than the RNA. Studies using this approach suggested that the minimum length of a DNA–RNA hybrid required for cleavage by *E. coli* RNase H1 is four nucleotides and that chimeric oligonucleotides with the 4-base deoxynucleotide gap in the middle or 5′ end of the hybridizing oligonucleotide (3′ end of the RNA substrate), but not those with the gap at the 3′ end, supported RNase H1 cleavage [22]. In another study, methylphosphonate oligonucleotides were unable to support RNase H1 activity when in a duplex. However, chimeric oligonucleotides comprised of methylphosphonate wings and a phosphodiester deoxynucleotide gap supported RNase H1 activity better than the parent phosphodiester compounds [23].

Given the importance of RNase H in the mechanisms of action of many antisense oligonucleotides [25–28], we have focused on phosphorothioate oligonucleotides and on developing chimeric

Abbreviations used: DTT, dithiothreitol; T_m, melting temperature for nucleic acid hybridization; gapmer, chimeric oligonucleotide.

* To whom correspondence should be addressed.

oligonucleotides that may have higher affinities for RNA targets yet still support RNase H activity. With this in mind, the objectives of the present study were to gain a more detailed understanding of the kinetic characteristics of RNase H, the effects of phosphorothioate oligonucleotides on these kinetic properties and to explore the structure–activity relationships that relate to the effects on RNase H. We have chosen to use *E. coli* RNase H1 because it is pure and well characterized and the enzymic mechanisms employed by *E. coli* RNase H1 appear to be comparable with those of mammalian enzymes.

MATERIALS AND METHODS

Materials

[γ-^{32}P]ATP (7000 Ci/mmol) was from ICN (Irvine, CA, U.S.A.). T4 polynucleotide kinase was purchased from Promega (Madison, WI, U.S.A.). Cytidine 3′,5′-[5′-^{32}P]bisphosphate triethylammonium salt ([^{32}P]pCp) was from Amersham/Life Sciences (Arlington Heights, IL, U.S.A.) with a specific radioactivity of 3000 Ci/mmol. T4 RNA ligase came from New England BioLabs (Beverly, MA, U.S.A.). Inhibit-Ace was from 5 Prime → 3 Prime (Boulder, CO, U.S.A.). *E. coli* RNase H was purchased from USB (Cleveland, OH, U.S.A.). Yeast tRNA was from Gibco BRL (Grand Island, NY, U.S.A.). The scintillation cocktail was Beckman 'Ready Safe' (Fullerton, CA, U.S.A.). RNase T_1 from *Aspergillus oryzae* was from Boehringer Mannheim, GmbH (Indianapolis, IN, U.S.A.).

Oligonucleotide synthesis

2′-*O*-Alkyl, 2′-fluoro and heterocyclic modified monomers were synthesized as described previously [25,29,30]. Syntheses of phosphorothioate (deoxy and 2′ modified) and phosphodiester oligonucleotides were performed using an Applied Biosystems 380B automated DNA synthesizer as described previously [25,29]. Purification of oligonucleotide products was also as described previously [25,29]. Purified oligonucleotide products were more than 90% full-length material as determined by PAGE. RNA substrates were further purified by PAGE (see below).

5′ Radiolabelling of the RNA oligonucleotide

The RNA oligonucleotide was 5′ end-labelled with [γ-^{32}P]ATP (7000 Ci/mmol) and 10 units of T4 polynucleotide kinase per 25 pmol of RNA. Incubation was performed at 37 °C for 1 h and stopped with 2× formamide loading buffer (90% formamide, 1× TBE (Tris-borate/EDTA), 0.25% Bromophenol Blue and 0.25% xylene cyanole). The labelled oligonucleotide was then gel-purified on 20% denaturing PAGE. The purified oligonucleotide was located by autoradiography, excised, and crushed in 0.3 M sodium acetate, pH 5.4, and then incubated at 37 °C for periods from 3 h to overnight. The supernatant was removed, precipitated with 2 vol. of ethanol, dried and resuspended in water. Specific radioactivity was between 1×10^6 c.p.m./ng and 4×10^6 c.p.m./ng.

3′ Radiolabelling of the RNA oligonucleotide

The RNA oligonucleotide was 3′ end-labelled with cytidine 3′,5′-[5′-^{32}P]bisphosphate (Amersham) and 15 units/ml T4 RNA ligase (New England BioLabs). Incubation was at room temperature overnight and the reaction was stopped with 2× formamide loading buffer. The oligonucleotide was then purified in the same fashion as the 5′-labelled oligonucleotide. Specific radioactivity was 6×10^4–3×10^5 c.p.m./ng.

Hybridization

At various concentrations, ranging from 12.5 nM to 250 nM, the radiolabelled RNA oligonucleotide was annealed with a 2-fold excess of the complementary strand in reaction buffer (pH 8.0) [20 mM Tris/HCl (pH 7.5), 20 mM KCl, 10 mM $MgCl_2$, 100 μM EDTA, 100 μM dithiothreitol (DTT)], and 1 unit of Inhibit-ACE per 10 μl final volume (final volume including enzyme dilution). Samples were heated to 65 °C for 5 min and then cooled slowly to room temperature or $\leqslant$ 30 °C. Complete hybridization of all the annealed duplexes was observed on 15% non-denaturing PAGE in 1× TBM buffer (1.12 M Tris base, 1.12 M boric acid and 10 mM $MgCl_2$). Unduplexed RNA was used as the control and the gels were analysed by autoradiography.

Determination of hybrid melting temperature (T_m)

Absorbance versus temperature profiles were measured on a Gilford Response spectrophotometer in buffer containing 100 mM Na^+, 10 mM phosphate (pH 7.1) and 0.1 mM EDTA at concentrations of each strand of 4 μM. T_m values of duplex formation were obtained from fits of data to a two-state model with linear sloping baselines [25,28]. Each value of T_m was derived from at least three experiments.

RNase H reactions

For each concentration of substrate, 2.6×10^{-9} mg of *E. coli* RNase H1 (USB, Cleveland, OH, U.S.A.) was incubated at 37 °C in a total volume of 100 μl of reaction buffer (20 mM Tris/HCl, pH 7.5, 20 mM KCl, 10 mM $MgCl_2$, 0.1 mM EDTA, 0.1 mM DTT). Aliquots (10 μl) were quenched at time points ranging from 0 to 360 s for deoxyphosphorothioates and 0 to 240 min for chimeric oligonucleotide ('gapmer') phosphorothioates. The aliquots were quenched with 22.2 mM EDTA and 0.56 mg/ml yeast tRNA on ice and then precipitated with 100 μl of 10% trichloroacetic acid for 5 min and then centrifuged, at 15000 ***g***, at 4 °C for 5 min. Aliquots (150 μl) of supernatant were removed and added to 2 ml of scintillation cocktail and the solubilized radioactivity analysed in a Beckman LS 5000TD scintillation counter. In addition, RNase H activity determination was analysed by PAGE. In this method, samples were quenched on ice in 10 μl aliquots of 2× formamide loading buffer. Samples were then heated at 95 °C for 4 min and loaded on to a 20% denaturing polyacrylamide gel and run in 1× TBE. Base (0.5 M sodium bicarbonate, pH 9.2) and RNase T_1-digested substrate samples were co-electrophoresed to provide oligonucleotide size markers. The gels were then analysed and quantified by phosphorimaging. The concentrations of substrates used ranged from 12.5 to 250 nM.

Kinetic analyses

Oligonucleotides were assayed by trichloroacetic acid precipitation over a range of concentrations ($n \geqslant 10$) to obtain K_m and $V_{max.}$. The Michaelis–Menten equation was applied and the K_m and $V_{max.}$ parameters were defined as previously described [31]. Kinetic analyses were also performed using polyacrylamide gel assays. To do this, each lane was scanned by a phosphorimager. The radioactivity in the intact band was divided by total radioactivity and then converted into concentration using the specific radioactivity. All assays were performed in the linear range of the phosphorimager.

RESULTS

Hybridization

To avoid inhibition of RNase H1 by higher concentrations of phosphorothioate oligonucleotides, antisense oligonucleotides and their RNA targets were prehybridized with only a 2-fold excess of the antisense oligonucleotides. Non-denaturing gel electrophoretic analyses were performed on all putative duplex substrates before enzymic analyses to assure full hybridization.

RNase H displays minimal sequence specificity and processively degrades RNA in phosphorothioate oligonucleotide duplexes

Figure 1 shows a polyacrylamide gel electrophoretic analysis of RNase H1 cleavage products from a 17-mer and a 20-mer RNA–phosphorothioate oligodeoxynucleotide duplex. This study shows several initial cleavage sites in each duplex target. Over time, it appears the nucleotides adjacent to the initial cleavage sites were degraded. Examination of cleavage products from these and other targets suggests that, although the enzyme might display a slight preference for guanosines, virtually no sequence preference was apparent. The final cleavage site was consistently 5–6 nucleotides from the 5′ terminus, suggesting that the enzyme requires approximately 5–6 DNA–RNA base pairs to effect cleavage. This may be due to either the space required for binding of the enzyme and/or loss of duplex structure. The cleavage site nearest the 3′ terminus of the duplex was 3–5 nucleotides from the terminus.

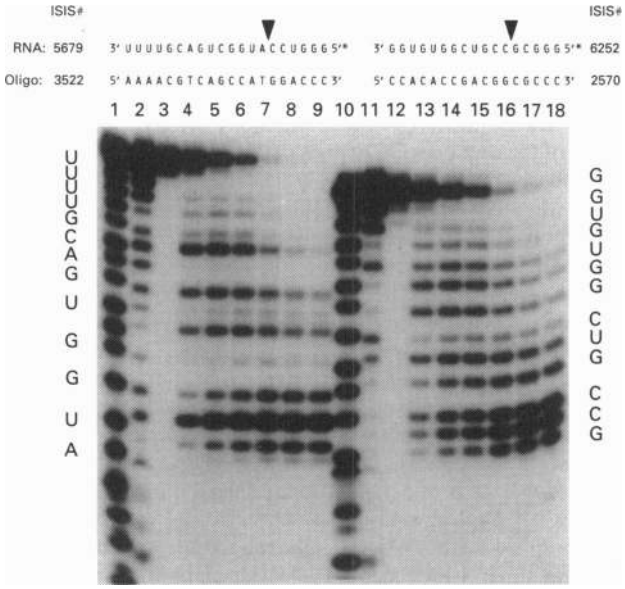

Figure 1 RNase H1 cleavage of two RNA–phosphorothioate-oligodeoxynucleotide duplexes

The 5′-labelled RNA species (indicated with an asterisk) shown at the top of the Figure were annealed with their appropriate phosphorothioate oligodeoxynucleotide complements, then incubated for various periods of time with *E. coli* RNase H1 as described in the Materials and methods section. The letters on the left- and right-hand sides of the Figure represent the sequence ladders for the corresponding RNA substrate. The arrowheads indicate the last cleavage site. On the left-hand side (lanes 1–9), the first two lanes are sizing ladders (alkaline and T1 RNase cleavage respectively) as described in the Materials and methods section, and the time points are as follows: 0, 20, 40, 60, 80, 120 and 240 s (lanes 3–9 respectively). On the right-hand side (lanes 10–18), the first two lanes (10 and 11) are ladders (OH^- and T1), as described in the Materials and methods section, and the time points are as follows: 0, 20, 40, 60, 80, 120 and 240 s (lanes 12–18 respectively).

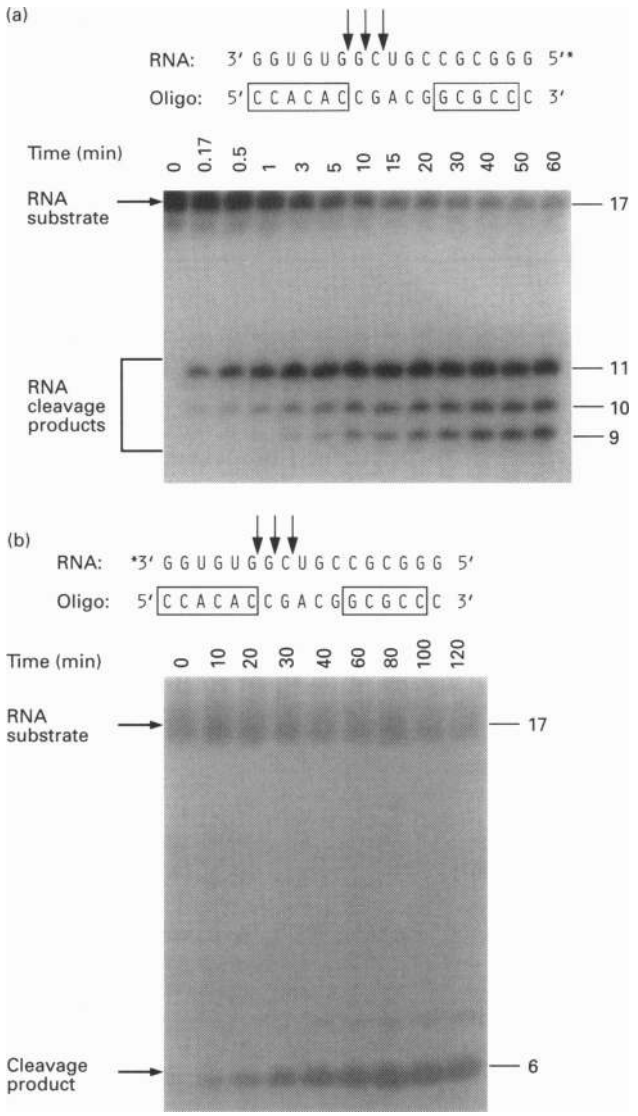

Figure 2 Kinetics of RNase H1 cleavage of an RNA–chimeric-oligonucleotide duplex

Hybridization, RNase H1 cleavage and gel electrophoretic analysis were performed as described in the Materials and methods section. Sequences for the RNA substrate and the antisense oligonucleotide are the same as those described in Figure 1 and are shown at the top of (**a**) and (**b**). Boxed sequences represent residues containing the 2′-methoxy sugar modification. The arrows above the RNA indicate the cleavage sites. The numbers at the right-hand side of the Figures represent the sizes (nt) of the RNA substrate or cleavage product, as determined by RNA sequence ladders. (**a**) Analysis of 5′-labelled RNA. (**b**) Analysis of 3′-labelled RNA.

To better assess processivity, we studied a duplex comprised of a 17-mer oligoribonucleotide and a phosphorothioate oligonucleotide with a centred 5-base 'deoxy gap' flanked with 2′-methoxy modifications. This size gap was selected to limit the number of initial cleavage sites to one and yet provide enough DNA–RNA duplex for the enzyme to display processivity. Figure 2(a) shows that 2′-methoxyoligonucleotides do not support RNase H activity (no cleavage observed in 2′-methoxy–RNA duplex regions). Similar results were reported when 2′-methoxynucleotides were incorporated in the RNA strand [22]. However, cleavage of the RNA target hybridized to the 2′-methoxy/deoxy chimera gap occurred. The initial site of cleavage occurred at the nucleotide adjacent to the methoxy–

Table 1 Kinetic constants for RNase H1 cleavage of two oligoribonucleotides duplexed to phosphorothioate oligodeoxynucleotides

Oligoribonucleotides were preannealed with the phosphorothioate oligodeoxynucleotides (17-mer or 20-mer) as shown in Figure 2. K_m and $V_{max.}$ values were determined as described in the Materials and methods section.

RNA sequence	K_m (nM)	$V_{max.}$ (μmol/min per mg)
3′-GGUGUGGCUGCCGCGGG-5′	44.8	27.2
3′-UUUUGCAGUCCCUACCUGGG-5′	36.4	40.4

deoxy junction closest to the 3′ end of the RNA substrate. Figure 2(a) also demonstrates processivity within the deoxy gap as the cleavage products increase with time in a 3′–5′ direction. Within a 5-base gap, three cleavages could be effected.

To confirm processivity further, two additional approaches were taken. First, Figure 2(b) shows the results of the same experiment as that described in Figure 2(a) except that the RNA substrate was labelled at the 3′ terminus rather than the 5′ terminus. If the enzyme is processive and not cleaving randomly, then PAGE analysis should show only one band of cleavage. The pattern of degradation was as predicted; there was a single band of cleavage at the expected site. Furthermore, adding excess competing duplex substrate at two time points (30 and 70 min after initiation of cleavage) had no effect on the rate of cleavage of adjacent nucleotides after cleavage was initiated, as would be expected if the enzyme were processive.

Kinetics of cleavage

Non-linear regression analyses were performed for two duplexes of different sequences and lengths (Table 1). The differences in the K_m and $V_{max.}$ are small and probably due to the fact that the 20-mer can accommodate at least one more enzyme molecule per molecule of substrate. It is highly unlikely that sequence played an important role since we and others [1] have not observed any sequence preference for *E. coli* RNase H1 (see Figure 2). To evaluate the potential effects of the phosphorothioate modifications on the efficiency of RNase H1 cleavage, we compared the initial rates between a uniform 17-mer phosphodiester and a uniform phosphorothioate oligodeoxynucleotide duplexed to an RNA complement. Surprisingly, the initial rate of cleavage of RNA in a duplex with the phosphodiester oligodeoxynucleotide was 15.7 nmol/min per mg ($r^2 > 0.994$) while that of the phosphorothioate-containing duplex was 33.9 nmol/min per mg ($r^2 > 0.99$). The units reported from these assays represent labelled nucleotides and oligonucleotides that are not precipitated by trichloroacetic acid. Under conditions employed in these studies, oligonucleotides shorter than 5-mers were not precipitated by trichloroacetic acid. This assay and these units have been used in previous studies on RNase H and, thus, our results can be compared directly with earlier work. We have also compared rates derived from trichloroacetic acid assays with those derived from PAGE analyses and found them to be similar. However, the trichloroacetic acid assay is most reproducible and each time point can be tested in triplicate, so it is a more quantitative assay.

We next examined the cleavage of duplexes comprised of 17- or 20-mer oligoribonucleotides and fully modified 2′-fluoro-, 2′-methoxy- and 2′-propoxy-phosphorothioate complements. No cleavage was observed under any conditions, including large excesses of RNase H1 and incubation times as long as 12 h (C. F. Bennett, N. M. Dean and B. P. Monia, unpublished work). Furthermore, uniform 2′-modified oligonucleotide–RNA duplexes did not affect the rate of RNase H cleavage of uniform deoxyoligonucleotide–RNA duplexes in competition experiments, indicating that the RNase H1 enzyme does not bind duplexes comprised of RNA hybridized with oligonucleotides uniformly modified at the 2′ sugar position (C. F. Bennett, N. M. Dean and B. P. Monia, unpublished work).

Table 2 compares the kinetic constants for duplexes formed with either a full oligodeoxynucleotide or oligonucleotides with 2′-methoxy wings and deoxynucleotide gaps 4 or 9 nucleotides in length. Clearly, although the 2′-methoxy wings increased the stability of the duplexes (T_m values of 73.9 °C and 67.6 °C for the 4- and 9-base chimeras respectively), cleavage of the RNA by the enzyme was substantially less efficient for chimeric duplexes. Furthermore, the larger gap supported more efficient cleavage than the shorter gap. To evaluate the effect of gap size in more detail, a series of gapmers from 1–9 nucleotides long was hybridized to the two oligoribonucleotides and the initial rates of cleavage by RNase H1 were determined. Table 3 shows that, as previously reported [21,22], a deoxy gap of four nucleotides is the minimum gap that will support *E. coli* RNase H1 activity. The initial rate of cleavage increased as the size of the gap increased.

To test the hypothesis that reduced cleavage efficiency in chimeric duplexes is due in part to a reduced number of enzyme molecules per duplex, a 43-mer RNA substrate was synthesized and hybridized with a 43-mer phosphorothioate complement containing three 4-base deoxynucleotide gaps interspersed be-

Table 2 Kinetic constants for RNase H1 cleavage of oligoribonucleotides duplexed with chimeric 2′-methoxy/deoxyphosphorothioate oligonucleotides

The sequence of the complementary antisense oligonucleotide is shown. The full deoxyphosphorothioate contains no 2′-methoxy modifications. The 2′-methoxyphosphorothioate/deoxy positions 7–10 chimera contains four consecutive centred deoxy residues. Similarly, the 2′-methoxyphosphorothioate/deoxy positions 5–13 chimera contains nine consecutive centred deoxy residues. Assay conditions and mathematical calculations were as described in the Materials and methods section.

Complement (5′-CCACACCGACGGCGCCC-3′)	K_m (nM)	$V_{max.}$ (μmol/min per mg)
Full deoxyphosphorothioate	44.8	27.2
2′-Methoxyphosphorothioate/deoxy positions 7–10	175.6	0.981
2′-Methoxyphosphorothioate/deoxy positions 5–13	245.6	3.09

Table 3 Effects of deoxynucleotide gap size on initial rates of cleavage of oligoribonucleotides

Sequences of the complementary phosphorothioate 2′-methoxy/deoxy chimera are shown in Figure 2 (17-mer and 20-mer). Deoxyoligonucleotide gap size indicates the length of the consecutive and centred deoxy residues in an otherwise uniform 2′-methoxyoligonucleotide complement. Assay conditions and mathematical calculations were as described in the Materials and methods section.

		Initial cleavage rates (nmol/min per mg)	
Deoxyoligonucleotide gap size	RNA sequence ...	3′-GGUGUGGCUGCCGCGGG-5′	3′-UUUUGCAGUCCCUACCUGGG-5′
1		Not detectable	Not detectable
3		Not detectable	Not detectable
4		7.89	7.18
5		9.57	11.5
7		–	21.0
8		26.8	–
9		–	46.0

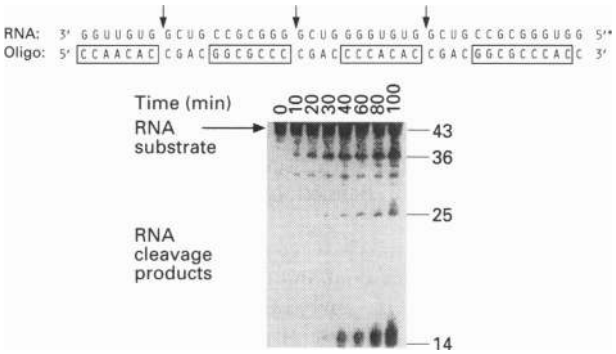

Figure 3 PAGE analysis of RNase H1 cleavage of a 43-mer RNA hybridized with a chimeric phosphorothioate oligonucleotide made up of four 2′-methoxy units each separated by a 4-base deoxynucleotide gap

The RNA and oligonucleotide were labelled and annealed as described in the Materials and methods section. The asterisks denote that the 5′ terminus of RNA is labelled. After annealing, the duplex was incubated with *E. coli* RNase H1 and aliquots were analysed by PAGE. As described, the arrows indicate points of cleavage. Lanes represent increasing time points (min) of RNase H1 cleavage. Sizes (nt) of RNA cleavage products and substrate are indicated on the right.

tween stretches of 2′-methoxynucleotides. Figure 3 shows the pattern of cleavage of this duplex showing three sites of cleavage. The K_m and $V_{max.}$ were 178.4 nM and 2.86 μmol/min per mg respectively. The K_m was nearly identical to that of the single 4-base gap, but the $V_{max.}$ was nearly 3-fold greater. This suggests that the decrement in K_m observed for the single gapmer compared with a full deoxynucleotide is related to the presence of the junction between the 2′-methoxy and deoxynucleotide portions of the chimera. The decrease in $V_{max.}$ in a gapmer compared with the full deoxynucleotide is due to the facts that each enzyme molecule is less efficient and fewer enzyme molecules per substrate are able to effect cleavage. We also studied the effect of gap placement on cleavage of RNA in a chimeric duplex. In contrast to a previous report [22], a deoxynucleotide gap at the 3′ terminus of the hybridizing oligonucleotide supported RNase H1 cleavage of RNA. The initial rate of cleavage was 0.404 nmol/min per mg. The oligonucleotide with the gap at the 5′ terminus supported no cleavage (C. F. Bennett, N. M. Dean and B. P. Monia, unpublished work).

The effects of several 2′ modifications incorporated into the wings of gapmers were also compared. To do this, a group of 5-base gapmers with either 2′-fluoro, 2′-methoxy or 2′-propoxy

Table 4 The effects of 2′ modifications on initial rates of RNase H1 cleavage of oligoribonucleotides

T_m values and initial rates for each compound were determined as described in the Materials and methods section. Each initial rate is the mean ± S.E.M. The number of determinations is shown in parentheses. The oligonucleotide sequence used was as follows: **CCACAC**CGACG**GCGCCC**; bold sequences represent sites in which 2′ modifications are incorporated.

Compound	T_m (°C)	Initial cleavage rate (nmol/min per mg)
Phosphodiester		
2′-Deoxy	67.9	15.72 ± 2.6 ($n = 5$)
2′-Propoxy	73.5	6.09 ± 3.8 ($n = 3$)
2′-Methoxy	77.2	4.94 ± 2.9 ($n = 5$)
Phosphorothioate		
2′-Deoxy	61.2	33.9 ± 2.0 ($n = 5$)
2′-Propoxy	67.8	6.23 ± 4.1 ($n = 3$)
2′-Methoxy	71.7	7.15 ± 1.9 ($n = 3$)
2′-Fluoro	79.0	7.15 ± 1.5 ($n = 5$)

wings in oligonucleotides containing phosphodiester or phosphorothioate backbones was synthesized and tested. As shown in Table 4, the relative affinities of the analogues for the RNA target were 2′-fluoro- ≫ 2′-methoxy- > 2′-propoxy- > 2′-deoxy-oligonucleotide, irrespective of whether the backbone was phosphodiester or phosphorothioate. However, the specific 2′ modification in the wings seemed to have only minimal effects on the initial rate of cleavage. All reduced the initial rate of cleavage relative to a fully deoxyoligonucleotide substantially, but the initial rates of the gapmers containing the various 2′ modifications were equivalent within experimental error.

Effects of base modifications on *E. coli* RNase H1 activity

To evaluate the effects of several base modifications, we inserted modified bases centred in a 5-nucleotide deoxynucleotide gap flanked with 2′-methoxy wings. Figure 4 shows the patterns of cleavage analysed by gel electrophoresis. Three adenosine modifications along with a 2′-methoxy nucleotide modification were studied. Modelling studies suggest that the N^6-imidazolylpropyl analogue protrudes into the major groove of the duplex and the N^2-imidazolylpropyl analogue protrudes into the minor groove. Therefore, these modifications were studied to provide preliminary insights into the effects of steric bulk on RNase H1 cleavage. The 2,6-diaminoadenosine analogues were selected to determine whether an increase in the stability of a base pair

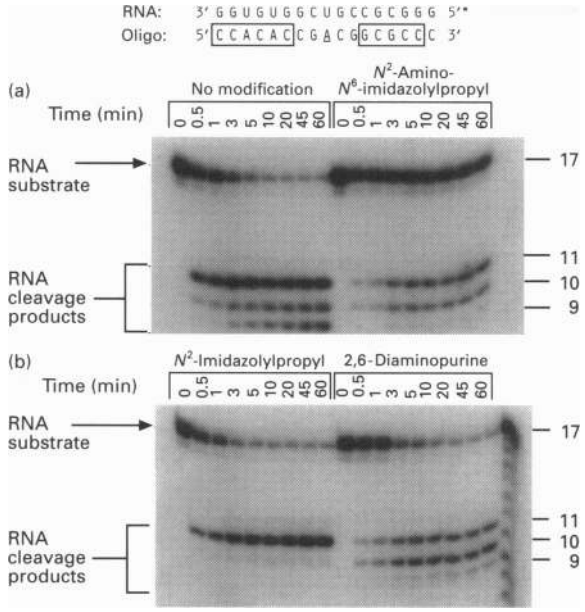

Figure 4 *E. coli* RNase H1 cleavage of RNA in a chimeric phosphorothioate duplex with modified adenosines in a deoxynucleotide gap

The complementary oligonucleotide to the 17-mer RNA target is shown at the top of the Figure (asterisk indicates 5′ terminus labelled), residues containing 2′-methoxy sugar modifications are boxed, deoxy sugars are not boxed, and the adenosine residue containing the indicated heterocycle modification is underlined. RNase H1 cleavage was performed for increasing times (min), as labelled, and cleavage products were analysed as described in the Materials and methods section. (**a**) Lanes 1–9, no modification; lanes 10–18, N^2-amino,N^6-imidazolylpropyl modification. (**b**) Lanes 1–9, N^2-imidazolylpropyl; lanes 10–18, 2,6-diaminopurine.

would influence the activity of RNase H1. We have found that this modification increases the T_m of this base pair by approximately +1 °C (E. A. Lesnik and S. M. Freier, unpublished work). As can be seen, the initial site of cleavage was unaffected by the presence of any of the base analogues in the gap. However, the rate of the initial cleavage event and the ability of the enzyme to processively degrade adjacent nucleotides within the deoxynucleotide gap were affected by the base modifications.

As can be seen in Figure 4, three cleavages were observed as expected in the gap with no modifications. In the N^6-imidazolylpropyladenosine-modified oligonucleotide, the rate of the first cleavage was less. The second cleavage was also inhibited, and the third cleavage was almost entirely inhibited. In contrast, while the N^2-imidazolylpropyladenosine had little to no effect on cleavage at the first cleavage site, all subsequent cleavages were inhibited. The 2,6-diaminopurine seemed to enhance the second cleavage relative to the initial cleavage. In fact, the pattern of cleavage suggests that the cleavages may not have been processive, but rather that the enzyme showed no preference for the site of cleavage adjacent to the junction of the deoxynucleotide gap. Additionally, the cleavage of the third site was inhibited, but the enzyme was able to effect the cleavage to some extent. Replacement of adenosine with 2′-methoxyadenosine essentially ablated all cleavage (C. F. Bennett, N. M. Dean and B. P. Monia, unpublished work).

Table 5 shows the initial cleavage rates for the unmodified gap and the oligonucleotides containing the 3-base analogues. As suggested by the PAGE analyses, the N^6-imidazolylpropyladenosine modification significantly inhibited the initial rate of cleavage, while the other two modifications had no effect. The initial rate measured for the N^2-imidazolylpropyladenosine-containing gapmer probably represented cleavage at two sites. The rates for the unmodified gapmer and the other two analogues represented cleavage essentially at the first site only. (Please note that the mean initial rate for the 5-base methoxy gapmer shown in Table 4 is 7.15±1.9 nmol/min per mg. In Tables 3 and 5, the initial rates determined in the specific experiments are shown to provide the most direct comparisons. Thus, the variation in initial rates over several months was minimal.)

In addition to the purine modifications, the effects of two modifications at the 5-position of pyrimidines were tested. Modifications of pyrimidines at the 5-position are of potential interest because they have been reported to enhance hybridization. In fact, 5-propynethymidine, when incorporated into antisense oligonucleotides, has been reported to increase affinity and antisense potency and support RNase H cleavage [32]. Similarly, 5-methylcytosine has been shown to increase the affinity of oligonucleotides for target RNAs (E. A. Lesnik and S. M. Freier, unpublished work). Thus, these two modifications

Table 6 The effects on hybridization and the initial rates of RNase H1 cleavage of oligoribonucleotides of modifications in the 5 position of pyrimidines

T_m values and initial rates were determined as described in the Materials and methods section. Each initial rate is the mean±S.E.M. The number of determinations is shown in parentheses. The sequence shown (CCACACCGACGGCGCCC) is the parent phosphorothioate oligonucleotide with the positions in which either 5-methyl- or 5-propynyl-cytosine was substituted underlined.

Modification	T_m (°C)	Initial cleavage rate (nmol/min per mg)
Parent	61.2	33.9±2.0 ($n=5$)
5-Propyne	74.9	37.9±4.2 ($n=3$)
5-Methyl	65.6	66.2±3.1 ($n=3$)

Table 5 Initial rates of RNase H1 cleavage of RNA duplexes with chimeric oligonucleotides containing adenosine base modifications

Sequences and chimeric design of the complementary phosphorothioate 2′-methoxy/deoxy chimeras and the position of the adenosine heterocycle modifications are shown in Figure 4(a). Initial rates were calculated from data in Figure 4 as described in the Materials and methods section.

Modification	ΔT_m/modification (°C)	Initial rate (nmol/min per mg)
None	–	7.12
N^6-Imidazoylpropyl-2-aminoadenosine	−0.20	2.86
N^2-Imidazoylpropyladenosine	0.84	8.12
2,6-Diaminopurine	0.95	7.02

were incorporated into the positions shown in Table 6, then evaluated. As shown in Table 6, both modifications enhanced affinity quite dramatically and supported RNase H1 cleavage. However, the 5-propyne modifications enhanced duplex stability more than the 5-methyl modifications. The antisense oligonucleotide in which 5-propynecytosine was incorporated supported an initial rate of cleavage equal to that of the parent phosphorothioate molecule. Interestingly, the initial rate of cleavage for the 5-methylcytosine-containing oligonucleotide was, in fact, nearly twice that of the parent phosphorothioate oligonucleotide.

DISCUSSION

This study confirms and extends a number of observations concerning the substrate specificity of *E. coli* RNase H. Oligoribonucleotides duplexed to phosphorothioate oligodeoxynucleotides are substrates that are effectively cleaved by the enzyme as reported previously [23]. Figure 1 demonstrates that *E. coli* RNase H1 exhibits virtually no sequence preference. As previously reported, 2′-methoxyoligonucleotides do not support RNase H1 activity when in an RNA-containing duplex [19,22,23,25,28]. As shown here, neither do 2′-fluoro- or 2′-propoxy-modified oligonucleotides. Thus, the 2′ position in the complementary 'antisense' strand is vital to RNase H activity.

That RNase H1 induces an endonucleolytic cleavage, then processively exonucleolytically degrades an RNA strand in a DNA–RNA duplex, has been reported previously [20]. The present study confirms that observation. As performed here, the use of gapmers or chimeric oligonucleotides to limit the number of enzyme molecules that can be bound per duplex substrate molecule enables unequivocal demonstration of this type of activity (Figure 2a). We confirmed processivity by using 3′-end-labelled RNA (Figure 2b). Moreover, competition experiments performed here provide further proof of processivity. Thus, the enzyme appears to require 4–6 nucleotides of a DNA–RNA duplex to bind and cleave effectively.

Kinetic parameters

The K_m and $V_{max.}$ values for the 17-mer and 20-mer RNA–phosphorothioate oligodeoxynucleotide duplexes were 48.4 nM and 27.2 μmol/min per mg and 36.4 nM and 40.4 μmol/min per mg respectively. These values are quite similar and the slight increase in $V_{max.}$ for the 20-mer duplex is probably due to the greater number of potential cleavage sites in the 20-mer duplex. The initial rate of RNA cleavage for a duplex comprised of a phosphorothioate oligodeoxynucleotide was actually greater than that of a duplex with a phosphodiester oligodeoxynucleotide. Thus, despite the fact that excess phosphorothioate oligonucleotides may inhibit the enzyme, the cleavage of RNA in a duplex containing a phosphorothioate oligonucleotide was at least equal to and apparently greater than in that containing a phosphodiester oligonucleotide. Consequently, the inhibition of the enzyme induced by phosphorothioates must result from binding of single-stranded phosphorothioate oligonucleotides to the enzyme. At present, we have no explanation for the apparent increase in initial cleavage rate caused by a phosphorothioate modification. As the phosphorothioate-containing duplex has a lower affinity, one possibility is that product release is more rapid, but this remains entirely speculative. The kinetic constants previously reported for the enzyme [16] are reasonably similar to those we have observed given the differences in conditions.

The cleavage of RNA in a 2′-modified chimeric duplex was substantially less efficient than in a duplex comprised of RNA–oligodeoxynucleotide. The K_m and $V_{max.}$ values were adversely affected even in a 9-base gap and, in a 4-base gap, the negative effects were even more pronounced. Moreover, initial rates determined for gapmers that varied from 1 to 9 deoxynucleotides showed a clear correlation between the size of the gap and the efficiency of cleavage. These studies confirm the fact that a minimum gap of four deoxynucleotides is required for cleavage of RNA by *E. coli* RNase H1 [22], but differ from a report that indicated that the presence of methoxy groups in wings had no effect on the efficiency of cleavage [21]. We ascribe this difference to two potential factors. First, in the previous reports, the 2′-methoxy substituents were made in the RNA strand. Placement of the 2′-methoxy groups in the wings of the DNA strand may reduce the enzyme affinity through unfavourable steric interactions as the enzyme binds to the minor groove of the duplex. In addition, the 2′-methoxy groups may alter the conformation of the duplex in a manner which reduces the efficiency of cleavage. The 2′-methoxy–RNA duplex has decreased flexibility compared with a DNA–RNA duplex, since the 2′-methoxy sugars strongly prefer the 'N' conformation (C3′ endo). If RNase H proceeds through an axial, in-line displacement of a 5′-phosphoryl leaving group, the enzyme is required to distort the local helical structure to bring the incipient nucleophile into proximity. Introduction of 2′-methoxy groups on either side of a deoxy gap would increase the energetic cost of producing this local distortion. As the number of deoxy residues in the gap is increased, the efficiency of cleavage would increase as the energetic penalty is diminished. A second, trivial possibility is that as the current studies were more detailed than those in the earlier report, the effects observed here were simply not identified. More work is required before a definitive conclusion can be made. As antisense oligonucleotides are designed to bind to RNA, clearly the results of our studies provide more relevant information for the design of antisense drugs. However, equally clearly, RNA can be methylated in the 2′ position. Thus, understanding the effects of RNA modifications, including 2′-*O*-methylation, may be important in the design of antisense oligonucleotides.

An additional important question in the design of optimal chimeric 2′-modified oligonucleotides is whether the nature of the 2′ modification affects RNase H cleavage. To address this, we studied a group of 2′-modified gapmers. Table 4 shows that the nature of the 2′ substituent in the wings of a gapmer has a significant influence on the affinity of the oligonucleotide for its target RNA, with the 2′-fluoro modification resulting in the greatest increase in affinity. However, all modifications induced an approximately equivalent reduction in the initial rates of cleavage. As a general rule, the more 'RNA-like' the antisense oligonucleotide, the more A-form the geometry of the duplex [33]. Thus, the T_m of the duplex formed with the 2′-fluoro chimera is significantly greater than that with the 2′-methoxy chimera which is greater than that with the 2′-propoxy or the 2′-deoxy parent oligonucleotide. Nevertheless, the initial rates of cleavage of all the 2′-modified oligonucleotides were equivalent. Thus, the enzyme clearly is not differentially affected by differences in the geometry of the duplexes in the wings or the junction. We can, therefore, conclude that the detrimental effects of the 2′ position modifications on the efficiency of cleavage by RNase H1 cannot be due to changes in the geometry of the duplex at the chimeric junction or in the wings. Nor can the effects of 2′ modifications on the efficiency of the enzyme be due to changes in the rate of denaturation of the duplex during or after cleavage. Rather, the effects of 2′ modifications must be due to a requirement of the enzyme to recognize the 2′-deoxy position in the antisense oligonucleotide.

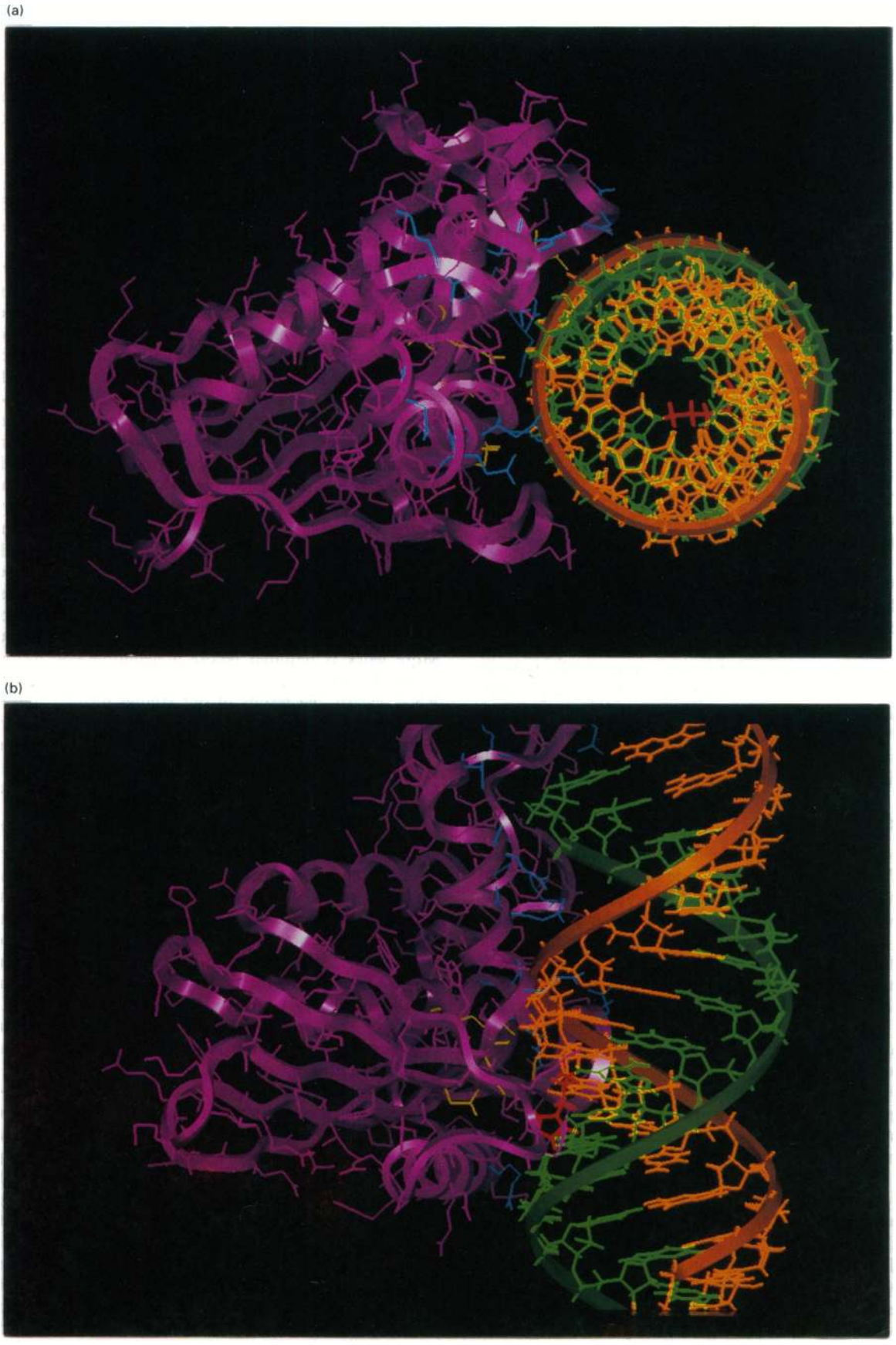

Figure 5 For caption, see facing page.

The effects of heterocycle modifications on cleavage of RNA by RNase H1

We inserted modified adenosines at the centre of a 5-nucleotide gap to begin to evaluate (i) the fine structure of the enzyme–substrate complex, (ii) the various steps in the cleavage process, (iii) the mechanisms underlying processivity and (iv) to begin the development of structure–activity relationships that might support the design of more effective antisense oligonucleotides. The N^2- and N^6-imidazolylpropyl modifications were selected because they are expected to protrude into the minor and major grooves of an RNA–DNA duplex respectively. Figure 5(a) presents a view down the helical axis of the RNA–DNA gapmer duplex docked to RNase H. The N^6-imidazolylpropyl group on the deoxynucleotide is highlighted in red and is situated in the major groove of the duplex. In this position, the modification cannot make contact with the enzyme. Figure 5(b) shows a view orthogonal to the helical axis of the N^2-imidazolylpropyl-deoxyadenosine duplex docked to RNase H. This modification, shown in red, is located in the minor groove of the duplex. While the local structure of the duplex is altered, the modification induces no major changes in the structure. Figure 4 and Table 4 show that the two modifications had very different effects on cleavage. The N^2 modification had no effect on the initial cleavage event, then obstructed all subsequent cleavages. Thus, the effects of this modification were transmitted at least two nucleotides from the modification, and the effects on the endonucleolytic first cleavage were clearly quite different from those on the exonucleolytic processive cleavages.

In contrast, the N^6 modification that is thought to protrude into the major groove inhibited the initial endonucleolytic cleavage event and increased the extent of the second cleavage relative to the initial cleavage. This could result either from 'slippage' of the enzyme, i.e. loss of selectivity for the initial endonucleolytic cleavage site, or different effects on the endonucleolytic versus exonucleolytic activities of the enzyme. Both modifications resulted in ablation of the enzyme's ability to cleave the ribonucleotide hybridized to the modified adenosine.

2,6-Diaminopurine was incorporated to evaluate the effects of a local increase in affinity of the duplex on the cleavage efficiency of the enzyme. In this case, we observed almost equal rates of cleavage of two adjacent nucleotides in the gap and significant inhibition of cleavage of the ribonucleotide hybridized to 2,6-diaminopurine. The inhibition may be due to a reduction in the off-rate of the products. However, studies with mismatched oligonucleotides showed only a slight reduction in cleavage rates (39.2 nmol/min per mg versus 20.8 nmol/min per mg for the perfectly matched duplex or the single mismatched duplex respectively). Thus, this seems unlikely. Alternatively, the inhibition of cleavage may result from increased energetic costs associated with local distortion of the helix.

We also evaluated the effects of modification in the 5 position of pyrimidines. Both 5-propyne and 5-methyl modifications increased the affinity of antisense oligonucleotides for complementary RNA, but the 5-methyl modification actually increased the initial rate of cleavage. Again, this demonstrates that it is possible to increase the stability of the duplex without adversely affecting the efficiency of the enzyme. At present, there are insufficient data to determine the reasons for the differences between the 5-propyne and 5-methyl modifications.

Therapeutic implications

Our laboratory and others [23,25,26,30] have designed antisense chimeras to enhance the affinity of antisense oligonucleotides for their RNA targets while retaining RNase H activity, in the hope of increasing the potency and specificity of antisense oligonucleotides. We have reported improved potency in the inhibition of Ha-*ras* that directly correlated with the increase in affinity [25]. However, for many other target sequences, we have failed to observe an increase in potency despite the proven increase in affinity. The current studies provide one possible explanation for these discrepant results. Clearly, the potency of an oligonucleotide dependent on an RNase H mechanism will be at least a function of the affinity of the oligonucleotide for its receptor sequence and the efficiency of the cleavage of the RNA by the enzyme. With current chimeric strategies, we are increasing affinity for target, but reducing efficiency of cleavage. We would suggest that when a current chimeric strategy is successful, binding of the oligonucleotide to its target RNA is rate limiting. When chimeric strategies fail to increase potency, the detrimental effects on the efficiency of cleavage must outweigh the benefits of enhanced affinity.

That the RNA in a phosphorothioate-oligonucleotide–RNA duplex is cleaved as efficiently or more efficiently than that in a phosphodiester duplex argues that the inhibitory activity of excess phosphorothioate oligonucleotides is due to the single-stranded phosphorothioate oligonucleotide. This suggests that substantial excess phosphorothioate may be detrimental if the terminating mechanism is RNase H degradation and suggests that well-considered dosing regimens will be essential to achieve optimal therapeutic utility for phosphorothioates.

This study also provides guidance with regard to selection of various modifications to incorporate into antisense oligonucleotides. As there is no significant difference in the effects of various 2′ modifications on the cleavage efficiency of the enzyme, all other things being equal, the 2′ modification that results in a maximal increase in duplex stability would be the modification of choice. Of the 2′ sugar modifications presented in this report, the 2′-fluorophosphorothioate would be the oligonucleotide of choice. The pyrimidines modified at the 5-position also offer increased affinity, but without detrimental effects on cleavage. Thus, these are also attractive modifications. Of the two pyrimidine modifications studied, the 5-methyl is perhaps more attractive than the 5-propyne because it appears to increase the cleavage rate. Additionally, as the potential for metabolism of oligonucleotides to toxic nucleosides must be considered, the fact that the 5-propyne-modified pyrimidines have been reported to be considerably more toxic than 5-methylcytosine [32] would also argue for the choice of 5-methyl-modified pyrimidines.

Figure 5 Representations of the RNase H–RNA–DNA gapmer complexes

(**a**) Structure of the 2,6-diaminoadenosine–RNase H–RNA–DNA gapmer duplex with an N^6-imidazoylpropyladenosine nucleotide looking down the helical axis. The crystal structure of *E. coli* RNase H was retrieved from the Protein DataBank. The backbone amide linkages are shown as ribbons to highlight the β-sheet and α-helix structures. The basic side-chains of the RNase H are coloured light blue, and the requisite glutamate carboxyl groups are presented as yellow. The structure of the rGGUGUGGCUGCCGCGGG:rCCACACcga*cgGCGCCC duplex (lower-case bases as deoxynucleotides) was generated from standard A-form RNA–DNA co-ordinates, the N^2 or N^6-imidazoylpropyl group was appended on to the deoxyadenosine in the structure and minimized for 100 ps using the Amber forcefield and Discover software. The RNA strand is shown in orange, while the DNA strand is coloured green. The imidazoylpropyl group appears red. The duplex was docked to the crystal structure to maximize the electrostatic and van der Walls potentials using the Biosym software package. Both views have been rotated to optimize visualization of the imidazoylpropyl side chain; (**b**) RNase H–RNA–DNA gapmer duplex with an N^2-imidazoylpropyl nucleotide viewed orthogonal to the helical axis.

We would like to thank Mary Ann Zounes and Pierre Villiet for oligonucleotide synthesis, Loren Miraglia and Henri Sasmor for technical advice and Colleen Matzinger for excellent typographical assistance.

REFERENCES

1 Hostomsky, Z., Hostomska, Z. and Matthews, D. A. (1993) in Nucleases (Linn, S. M., Lloyd, R. S. and Roberts, R. J., eds.), pp. 341–376, Cold Spring Harbor Laboratory, Cold Spring Harbor, NY
2 Itaya, M. (1990) Proc. Natl. Acad. Sci. U.S.A. **87**, 8587–8591
3 Itaya, M. and Kondo, K. (1991) Nucleic Acids Res. **19**, 4443–4449
4 Itaya, M., McKelvin, D., Chatterjie, S. K. and Crouch, R. J. (1991) Mol. Gen. Genet. **227**, 438–445
5 Kanaya, S. and Ktaya, M. (1992) J. Biol. Chem. **267**, 10184–10192
6 Karwan, R., Blutsch, H. and Wintersberger, U. (1983) Biochemistry **22**, 5500–5507
7 Campbell, A. G. and Ray, D. S. (1993) Proc. Natl. Acad. Sci. U.S.A. **90**, 9350–9354
8 Busen, W. (1980) J. Biol. Chem. **255**, 9434–9443
9 Rong, Y. W. and Carl, P. L. (1990) Biochemistry **29**, 383–389
10 Eder, P. S., Walder, R. Y. and Walder, J. A. (1993) Biochimie **75**, 123–126
11 Tanese, N. and Goff, S. P. (1988) Proc. Natl. Acad. Sci. U.S.A. **85**, 1777–1781
12 Ben-Artzi, H., Zeelon, E., Zmit, B., Wortzel, A., Gorecki, M. and Panet, A. (1993) J. Biol. Chem. **268**, 16465–16471
13 Katayanagi, K., Miyagawa, M., Matsushima, M., et al. (1990) Nature (London) **347**, 306–309
14 Yang, W., Hendrickson, W. A., Crouch, R. J. and Satow, Y. (1990) Science **249**, 1398–1405
15 Katayanagi, K., Miyagawa, M., Matsushima, M., et al. (1992) Mol. Biol. **223**, 1029–1052
16 Kanaya, S., Katsuda-Nakai, C. and Ikehara, M. (1991) J. Biol. Chem. **266**, 11621–11627
17 Nakamura, H., Oda, Y., Iwai, S., et al. (1991) Proc. Natl. Acad. Sci. U.S.A. **88**, 11535–11539
18 Furdon, P. J., Dominski, Z. and Kole, R. (1989) Nucleic Acids Res. **17**, 9193–9204
19 Eder, P. S., Walder, R. Y. and Walder, J. A. (1993) Biochimie **75**, 123–126
20 Schatz, O., Mous, J. and Le Grice, S. F. J. (1990) EMBO J. **9**, 1171–1176
21 Hogrefe, H. H., Hogrefe, R. I., Walder, R. Y. and Walder, J. A. (1990) J. Biol. Chem. **265**, 5561–5566
22 Inoue, H., Hayase, Y., Iwai, S. and Ohtsuka, E. (1988) Nucleic Acids Res. **19**, 135–138
23 Giles, R. V. and Tidd, D. M. (1992) Anti-Cancer Drug Design **7**, 37–48
24 Reference deleted
25 Monia, B. P., Lesnik, E. A., Gonzalez, C., et al. (1993) J. Biol. Chem. **268**, 14514–14522
26 Mirabelli, C. K. and Crooke, S. T. (1993) in Antisense Research and Applications (Crooke, S. T. and Lebleu, B., eds.), pp. 15–35, CRC Press, Inc., Boca Raton, FL
27 Gao, W.-Y., Han, F.-S., Storm, C., Egan, W. and Cheng, Y.-C. (1992) Mol. Pharmacol. **41**, 223–229
28 Chiang, M.-Y., Chan, H., Zounes, M. A., Freier, S. M., Lima, W. and Bennett, C. F. (1991) J. Biol. Chem. **266**, 18162–18171
29 Guinosso, C. J., Hoke, G. D., Freier, S. M., et al. (1991) Nucleosides Nucleotides **10**, 259–262
30 Ramasamy, K. S., Zounes, M. A., Gonzalez, C., et al. (1994) Tetrahedron Lett. **35**, 215–218
31 Henderson, P. J. F. (1992) in Enzyme Assays: A Practical Approach (Eisenthal, R. and Danson, M. J., eds.), pp. 277–316, Oxford University Press, New York
32 Wagner, R. W., Matteucci, M. D., Lewis, J. G., Gutierrez, A. J., Moulds, C. and Froehler, B. C. (1993) Science **260**, 1510–1513
33 Griffey, R. H., Lesnik, E. A., Freier, S., et al. (1994) in Carbohydrate Modifications in Antisense Research (Sanghvi, Y. S. and Cook, P. D., eds.), pp. 212–224, American Chemical Society, Washington, DC

Received 6 April 1995/10 July 1995; accepted 27 July 1995